

## **RECENT ADVANCES IN STRENGTHENING AND REINFORCING TECHNOLOGIES FOR PAPER DOCUMENTS: A COMPREHENSIVE REVIEW**

BY JING LANG, JIANJUN ZHOU, ZHENZHONG TANG, AND JIANHUI ZHANG

## **POLYETHYLENE GLYCOL/WOOD FLOUR PHASE CHANGE MATERIALS INCORPORATED INTO BIODEGRADABLE WOOD PLASTIC COMPOSITES FOR THERMAL ENERGY STORAGE**

BY LI XUELI, ZHANG YAOYI, ZHU LIZHI, FU ZHIQIANG, SONG SHUAIHAO, AND WU JING

## **BEHAVIOR OF BOLTED BEAM-TO-COLUMN TIMBER CONNECTIONS USING DOUBLE STEEL PLATES**

BY YOSAFAT AJI PRANATA AND BAMBANG SURYOATMONO

## **THE ANISOTROPIC VELOCITY MODEL OF INTERNAL ACOUSTIC EMISSION SIGNALS IN ZELKOVA WOOD AND THE INFLUENCE OF HOLES ON THEIR PROPAGATION PROCESS**

BY ZHIYING TIAN, SAIYIN FANG, MING LI, TINGTING DENG, ERZHUANG ZHAI, CHUMIN CHEN, AND YONGCHUAN WU

## **ANISOTROPIC PROPAGATION CHARACTERISTICS OF ACOUSTIC EMISSION SIGNALS IN WOOD**

BY YONGCHUAN WU, SAIYIN FANG, MING LI, TINGTING DENG, CHUMIN CHEN, AND ZHIYING TIAN

## **SURFACE PROPERTIES OF HYDRO-THERMALLY MODIFIED BEECH WOOD AFTER RADIO-FREQUENCY DISCHARGE PLASMA TREATMENT**

BY JÁN SEDLIAČIK, PAVLO BEKHTA, IGOR NOVÁK, ANGELA KLEINOVÁ, MATEJ MIČUŠÍK, JÁN MATYAŠOVSKÝ, AND PETER JURKOVIČ

## **MODELLING OF BIRCH WOOD (BETULA SPP.) SURFACE ROUGHNESS DEPENDING ON LASER PROCESSING PARAMETERS WITH RESPONSE SURFACE METHODOLOGY**

BY ÇAĞATAY ERSİN AND MEHMET GÜNEŞ

## **PREPARATION OF ECO-FRIENDLY COMPOSITE PAPER WITH GINKGO LEAF AND BIO-BASED FIBERS**

BY ZIXING MA, MENG ZHOU, YANGYI WANG, QIYUE WANG, HELAN XU, AND XIULIANG HOU

## **PULPING AND PAPERMAKING POTENTIAL OF ACACIA AULACOCARPA BENTH WOOD IN INDONESIA**

BY GANIS LUKMANDARU, MUHAMMAD AKBAR FAQIH, AND SIGIT SUNARTA

## **EFFECT OF ALKALINE TREATMENT ON MORPHOLOGY AND BIODEGRADATION OF BAGASSE AND MAIZE CELLULOSE**

BY TSHWAFO ELIAS MOTAUNG, ELLA CEBISA LINGANISO-DZIIKE, ZIKHONA TETANA, LEHLOHONOLO FORTUNE KOAO, AND SETUMO VICTOR MOTLOUNG

## **THE EFFECT OF UV ABSORBERS ON THE LIGHTFASTNESS OF DYED VENEERS**

BY LI LILI, LIU WENWEN, LUO ZHIYING, LIU DE, YU JIANFANG, WANG XIMING, ZHANG GUO, AND ZHEN JING RU

## **STUDY ON THE HYDROTHERMAL TREATMENT OF KILN-DRIED TIMBER OF RED ALDER**

BY LIN YANG, PUYAN ZHAO, AND QIN YIN

## **EFFECT OF SUPERCRITICAL CO<sub>2</sub> DEHYDRATION TREATMENT ON THE JUGLANS MANDSHURICA**

BY LIN YANG, HONGWEI FAN, AND JINGTING ZHENG

## **CHEMICAL CHANGES DURING WOOD CUTTING**

BY TAMAS HOFMANN, LASZLO TOLVAJ, AND ZOLTAN PASZTORY

## **SHORT NOTES. INFLUENCE OF WOOD ANATOMY ON THE DISTRIBUTION OF GUANIDINE BASED FIRE RETARDANTS IN FIVE FAST GROWING JAPANESE HARDWOODS**

BY CHUN-WON KANG, MASUMI HASEGAWA, KAWANISHI MARIA, AND HARADHAN KOLYA

## **BEHAVIOR OF BOLTED BEAM-TO-COLUMN TIMBER CONNECTIONS USING DOUBLE STEEL PLATES**

YOSAFAT AJI PRANATA  
UNIVERSITAS KRISTEN MARANATHA  
INDONESIA

BAMBANG SURYOATMONO  
UNIVERSITAS KATOLIK PARAHYANGAN  
INDONESIA

(RECEIVED APRIL 2025)

### **ABSTRACT**

This study aims to investigate the behavior of bolted beam-to-column timber connections with double steel plates. The behavior of the connections, as their strength, initial rotational stiffness, energy dissipation, and ductility ratio, were studied. Test specimens made of red meranti species (*Shorea spp.*) connected by 5-mm thick steel plates on both sides, and bolted joints of diameters 10 mm and 12 mm were used. Experimental tests of the connections conform to the EN 26891: 1991. The failure mode is splitting of the bolt row path in the column for all connections with the same numbers of bolts in the beam and the column, and splitting of the bolt row path in the beam for all connections with fewer numbers of bolts in the beam than those in the column. Moreover, the results show that the use of combined bolts and double steel plates has an impact in increasing both the ductility ratio and the energy dissipation of the connections.

**KEYWORDS:** Beam-to-column, connection, strength, ductility ratio, energy dissipation.

### **INTRODUCTION**

Hwang et al. (2008) in their study require rotational stiffness parameters for modeling traditional Korean building structures to support the research objective, namely the most exact structural behavior of real structures. Santana and Mascia (2009) also require parameters for modeling moment-resisting connectors, with the aim of studying the behavior of wooden-frame buildings. In engineering practice, the sound design of the load-bearing structure is as important as the sound design of the structural connections (Neusch et al. 2022). However, timber-framed

structures with semi-rigid joints of moment-resisting type have lower spatial stiffness behavior than theoretical models with full-fixed joints (Baszen and Miedzialowski 2019).

Moment-resisting type of connections in multi-story timber buildings utilize bolts with the aim of making the connection behave ductile (Fairweather 1992, Guo and Shu 2019). The use of steel plates as connecting parts can potentially have an impact, namely increasing the ductility of the connection system. In a structural analysis, establishing the moment and rotation relationship of the connection greatly determines the accuracy of the analysis.

Mehra et al. (2022, 2019) conducted research to study the beam-to-column timber connection with compressed wood connectors utilizing several variations of connection types, with the aim of investigating the rotational stiffness, moment capacity, and ductility ratio of the connection. The research method uses experimental testing with a monotonic loading method referring to the EN 26891: 1991. Solariano et al. (2017) conducted research to study the semi-rigid beam-to-column connection with steel dowels, with a monotonic loading method. The study used an experimental method with the results in the form of empirical data on the behavior of moment and rotational stiffness. Reboucas et al. (2022) has conducted review of the most important research studies that have focused on ductile beam-to-column connections in the moment-resisting timber frame system. Vilguts et al. (2022) conducted research to investigate the semi-rigid beam-to-column moment-resisting timber connections to quantify rotational stiffness, energy dissipation and moment resistance.

The modulus of toughness is a material property that quantifies its ability to absorb energy (energy dissipation) in plastic deformation before failure (Hibbeler 2023, Goodno and Gere 2021), represented by the area under the stress-strain curve up to the failure point (Fig. 1a). Similar definition is applied in bending moment versus rotation in a connection, the area under which represents the ability of the connection to dissipate energy. Proportional or yield load is the point at which the behavior of the specimen changes from elastic to post-elastic conditions due to incremental loads applied to the specimen. Determining the proportional load in this research uses the 5%-diameter offset method (ASTM 2018, Munoz et al. 2008) (Fig. 1b).

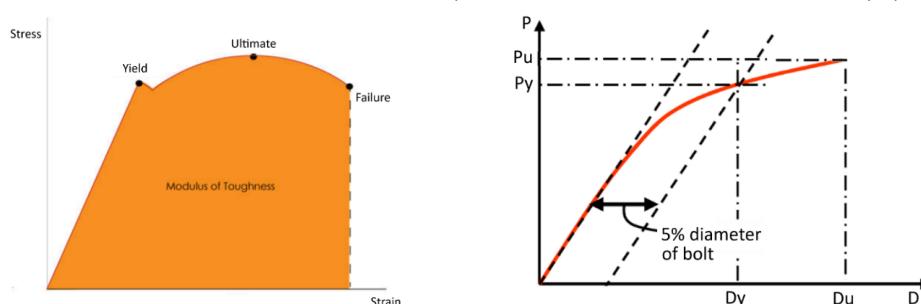


Fig. 1: a) An illustration of the area in the context of toughness modulus, b) the 5%-offset diameter method according to ASTM 2018,  $P_y$  represents the yield load,  $P_u$  represents the peak load,  $D_y$  corresponds to the displacement at  $P_y$ , while  $D_u$  corresponds to the displacement at  $P_u$ .

This study aims to investigate the behavior of bolted beam-to-column timber connections with double steel plates as connecting parts observing four parameters, namely strength, initial rotational stiffness, energy dissipation, and ductility ratio. This study focuses on the connection behavior needed in designing earthquake-resistant building, namely strength, initial rotational stiffness, energy dissipation, and ductility ratio.

## MATERIAL AND METHODS

The experimental tests in the laboratory to obtain empirical data and information on the behavior of bolted beam-to-column timber connections with double steel plates refer to EN 26891: 1991. An universal testing machine (Hung Ta 2008) was used and each specimen was loaded with the crosshead speed of 0.003 mm/min (displacement controlled).

The connecting parts of the beam-to-column connection are double steel plates, each of which has thickness of 5 mm. Fig. 2 shows the dimensions of the beam-to-column connection type 1 (3 bolts in the column and 2 bolts in the beam) for bolt diameters of 10 mm and 12 mm, respectively. Meanwhile, Fig. 3 shows the dimensions of the connection type 2 (3 bolts in the column and 3 bolts in the beam). Therefore, there were totally 12 beam-to-column specimens in this study. The beams and columns, made of red meranti (*Shorea spp.*), have a rectangular cross-section, with cross-sectional dimensions of 50 mm x 100 mm (Tab. 1).

Tab. 1: Specimen description.

Specimen type	Bolt diameter (mm)	Number of bolts		Number of specimens
		on column	on beam	
Type 1-BC32.10	10	3	2	3
Type 2-BC33.10			3	
Type 1-BC32.12	12		2	
Type 2-BC33.12			3	

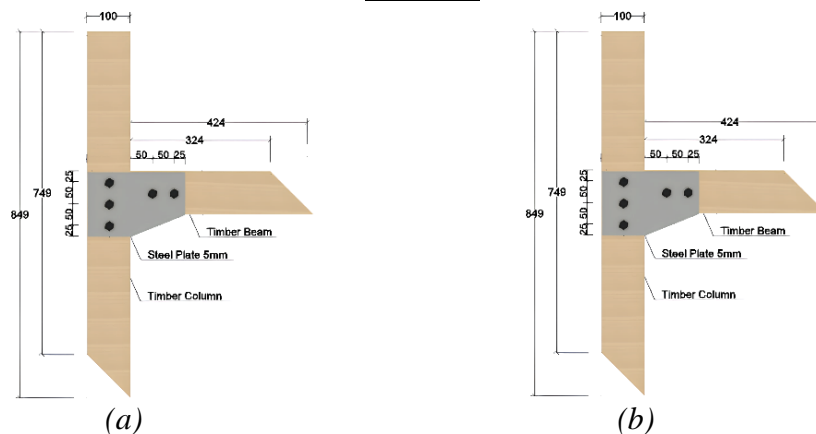


Fig. 2: Specimen dimensions of connection type 1 (a) BC32.10 and (b) BC32.12.

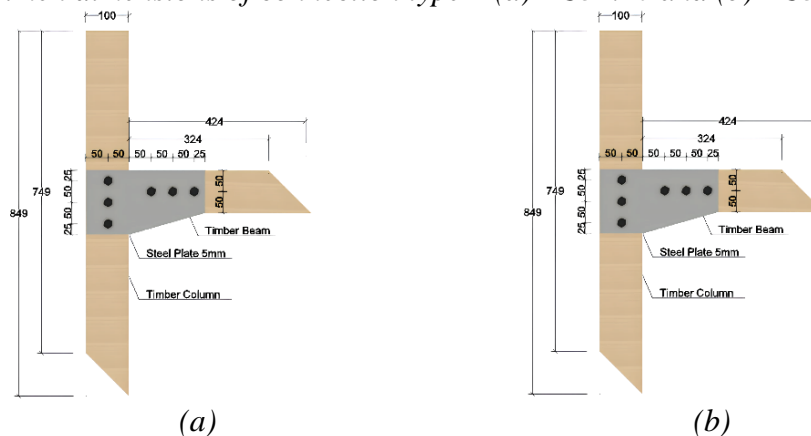


Fig. 3: Specimen dimensions of connection type 2 (a) BC33.10 and (b) BC33.12.

## RESULTS AND DISCUSSION

The test results are initially load and displacement relationships and later are converted into moment and rotation relationships. Fig. 4a shows the test setup of type 1 beam-to-column connections with 10 mm diameter bolts. Fig. 4b shows the test setup of type 2 connections with 10 mm diameter bolts. Fig. 4c shows the test setup of connections type 1 with 12 mm diameter bolts, and Fig. 4d shows the test setup of connections type 2 with 12 mm diameter bolts. The test uses incremental loading until the specimen fails.

Fig. 5 shows the failure pattern of specimens. The general failure modes for connections type 1 are splitting in the bolt row path in the beam and for connections type 2 are splitting on the bolt row path in the column. Experimental tests show that the bolt diameter does not alter the failure modes. In all specimens tested, there was no failure of the steel plate, neither in the form of bearing failure nor tear-out failure. Furthermore, all specimens tested show that there was no failure of the bolt, neither in the form of shear failure nor flexural yielding.

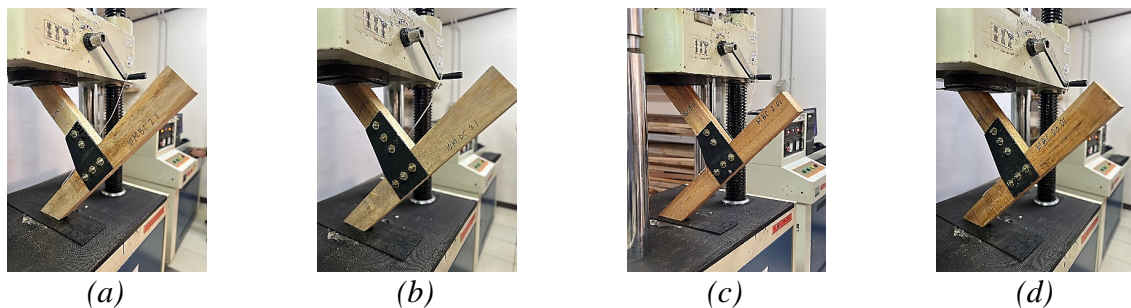


Fig. 4: Tests of connections (a) type 1-BC32.10, (b) type 2-BC33.10, (c) type 1-BC32.12, and (d) type 2-BC33.12.

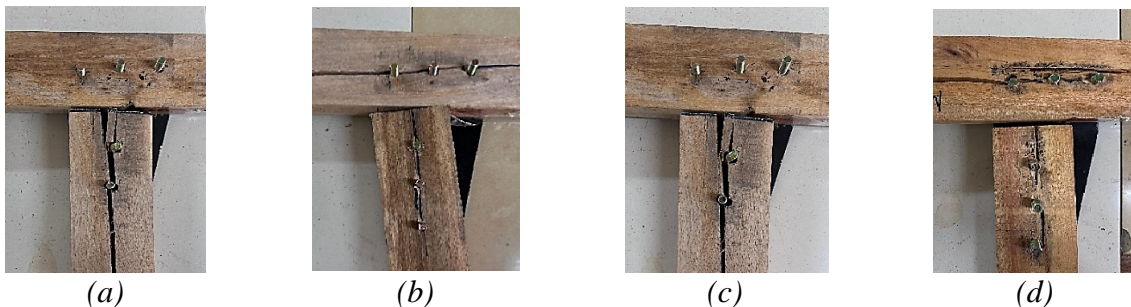


Fig. 5: Failure patterns of connections (a) type 1-BC32.10, (b) type 2-BC33.10, (c) type 1-BC32.12, and (d) type 2-BC33.12.

The test results in the form of the complete load and displacement curves, are shown in Fig. 6. The loads and displacements at the proportional (yield) and ultimate (peak) points are determined using the 5%-diameter offset method (ASTM 2018, Munoz 2008). The bending moment and rotation curves are calculated and shown in Fig. 7.



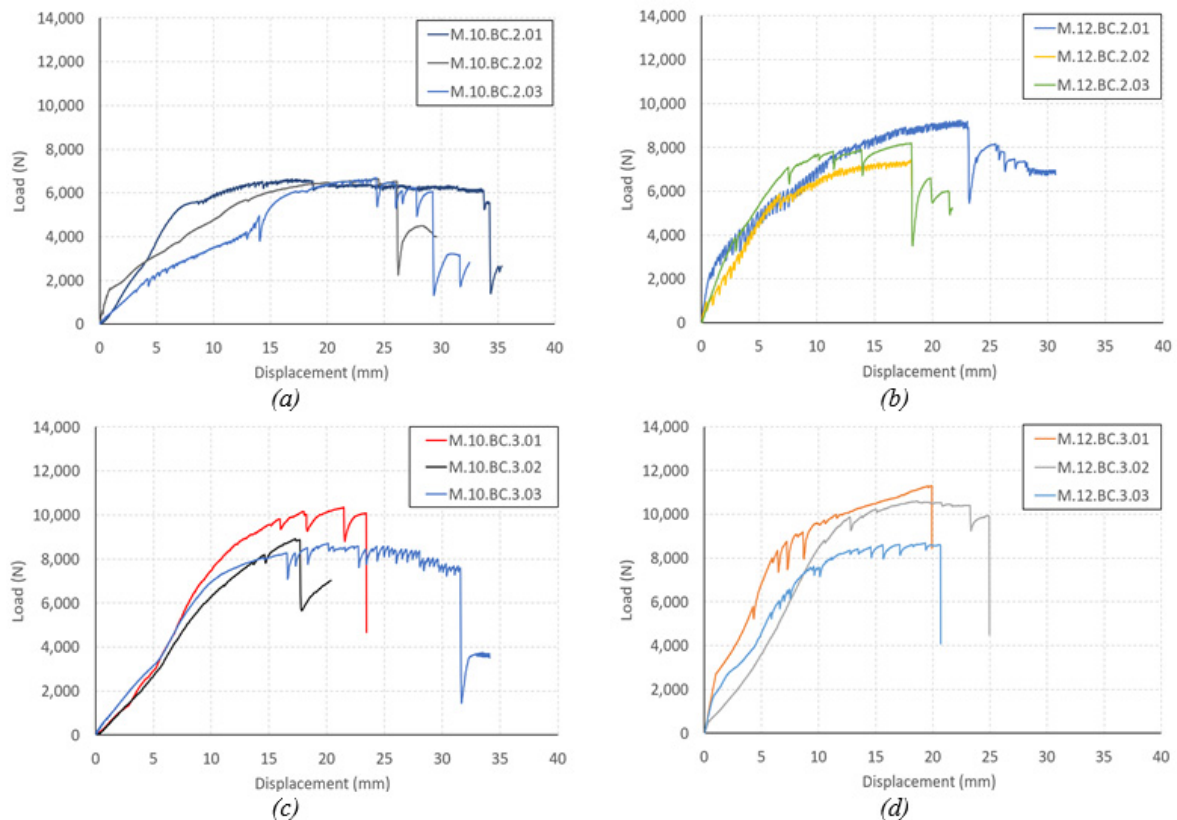


Fig. 6: Results of load and displacement curves of type 1 (a) BC32.10 and (b) BC32.12 and type 2 (c) BC33.10 and (d) BC33.12.

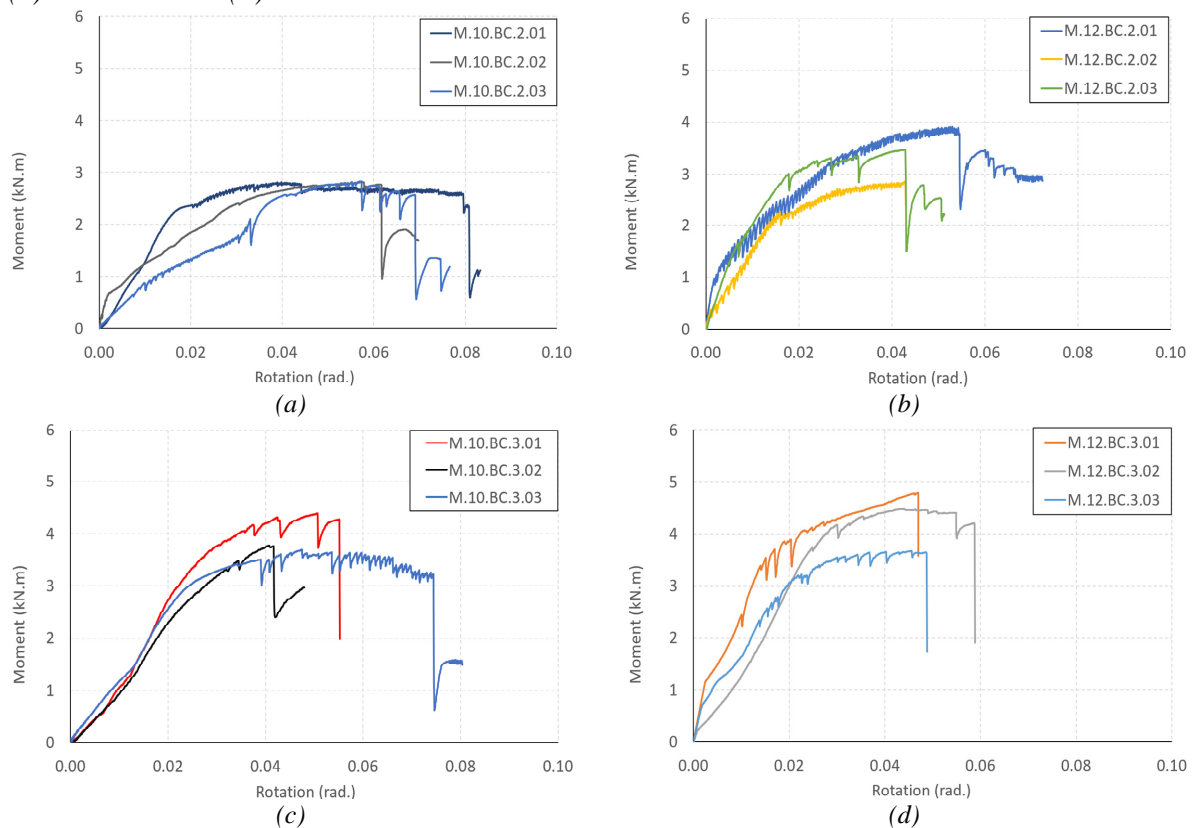


Fig. 7: Results of moment and rotational curves of type 1 (a) BC32.10 and (b) BC32.12 and type 2 (c) BC33.10 and (d) BC33.12.

Initial stiffness is calculated as the slope of the line in the elastic loading range of load and displacement relationship. The energy dissipation is calculated as the area under the moment and rotation curve ( $M-\theta$ ). The calculations of strength ( $M_u$  or moments in term of peak load) and ductility ratio are shown in Tab. 2. As seen in the ductility ratio ( $D_u/D_y$ ) of all specimens is in the range between 1.53 and 2.64. It is obvious that such relatively high ductility ratio is due to the presence of the bolts and the steel plates. The initial stiffness and energy dissipation for each specimen tested in this study is shown in Tab. 3 and Tab. 4, respectively.

*Tab. 2: Results obtained from experimental tests on specimens.*

Type 1-BC32.10									
Specimen	$P_y$ (N)	$D_y$ (mm)	$P_u$ (N)	$D_u$ (mm)	$M_y$ (kN.m)	$\theta_y$ (rad.)	$M_u$ (kN.m)	$\theta_u$ (rad.)	$\mu$ (-)
Specimen 1	5684.02	13.18	6422.78	25.93	2.41	0.0311	2.72	0.0612	1.97
Specimen 2	5472.74	8.68	6420.05	18.93	2.32	0.0205	2.72	0.0446	2.18
Specimen 3	5681.71	15.71	6682.51	24.30	2.41	0.0371	2.83	0.0573	1.55
Average	5612.82	12.52	6508.45	23.05	2.38	0.0295	2.76	0.0544	1.84
Type 2-BC33.10									
Specimen	$P_y$ (N)	$D_y$ (mm)	$P_u$ (N)	$D_u$ (mm)	$M_y$ (kN.m)	$\theta_y$ (rad.)	$M_u$ (kN.m)	$\theta_u$ (rad.)	$\mu$ (-)
Specimen 1	8791.37	12.48	9895.28	22.36	3.73	0.0294	4.20	0.0527	1.79
Specimen 2	8281.87	15.15	8351.58	23.22	3.51	0.0357	3.54	0.0548	1.53
Specimen 3	7222.13	10.67	887.44	17.66	3.06	0.0252	0.38	0.0417	1.66
Average	8098.46	12.77	6378.10	21.08	3.43	0.0301	2.70	0.0497	1.65
Type 1-BC32.12									
Specimen	$P_y$ (N)	$D_y$ (mm)	$P_u$ (N)	$D_u$ (mm)	$M_y$ (kN.m)	$\theta_y$ (rad.)	$M_u$ (kN.m)	$\theta_u$ (rad.)	$\mu$ (-)
Specimen 1	7424.57	10.19	8820.32	23.07	3.15	0.0240	3.74	0.0544	2.26
Specimen 2	6144.21	9.06	6973.18	18.23	2.61	0.0214	2.96	0.0430	2.01
Specimen 3	6932.45	7.84	8188.35	18.15	2.94	0.0185	3.47	0.0428	2.32
Average	6833.74	9.03	7993.95	19.82	2.90	0.0213	3.39	0.0467	2.19
Type 2-BC33.12									
Specimen	$P_y$ (N)	$D_y$ (mm)	$P_u$ (N)	$D_u$ (mm)	$M_y$ (kN.m)	$\theta_y$ (rad.)	$M_u$ (kN.m)	$\theta_u$ (rad.)	$\mu$ (-)
Specimen 1	8527.91	7.55	11307.10	19.94	3.62	0.0178	4.79	0.0470	2.64
Specimen 2	9718.47	13.36	10404.11	23.25	4.12	0.0315	4.41	0.0548	1.74
Specimen 3	7231.82	10.10	8564.18	20.68	3.07	0.0238	3.63	0.0488	2.05
Average	8492.73	10.34	10091.80	21.29	3.60	0.0244	4.28	0.0502	2.06

$P_y$  is the yield load,  $P_u$  is the peak load,  $D_y$  is the displacement at yield point, and  $D_u$  is the displacement at peak point,  $\mu$  is ductility ratio ( $D_u/D_y$ ).

*Tab. 3: Initial stiffness obtained from experimental tests.*

Specimen	Type 1-BC32.10 (N/mm)	Type 1-BC32.12 (N/mm)	Type 2-BC33.10 (N/mm)	Type 2-BC33.12 (N/mm)
Specimen 1	936.02	1106.63	1449.89	2640.78
Specimen 2	681.44	1122.06	1460.86	2123.44
Specimen 3	526.00	929.94	869.41	2259.60
Average	714.49	1052.88	1260.05	2341.27

*Tab. 4: Energy dissipation obtained from experimental tests.*

Specimen's	Type 1-BC32.10 (J)	Type 1-BC32.12 (J)	Type 2-BC33.10 (J)	Type 2-BC33.12 (J)
Specimen 1	189.33	210.60	160.04	165.61
Specimen 2	143.89	97.80	141.00	189.34
Specimen 3	137.70	133.36	216.32	135.18
Average	156.98	147.25	172.45	163.38



However, as shown in Fig. 8, the ductile behavior is also contributed by the fact that the column has sufficient compression strength perpendicular to the direction of the wood grain and in turn it can withstand the rotation of the beam.



Fig. 8: Embedment failure in compression perpendicular to the grain (a) in type 1 connections, (b) in type 2 connections.

## Discussion

In the last twenty years, performance-based seismic design for buildings has been developed (Padalu et al. 2023, Ponzo et al. 2021), especially for buildings with moment-resisting frames structural systems. In the design of multi-story timber buildings with this method, the capacity curve is a representation of the strength of the structure and it requires the actual behavior of the beam-to-column connection. Beam-to-column connections with a high level of energy dissipation can have an impact on the behavior of ductile structural stiffness (Casciati 2007).

Based on previous researches, red Meranti timber (*Shorea spp.*) has a bearing strength in the direction parallel to the wood grain of 32.74 MPa (Pranata and Suryoatmono 2024), compression strength perpendicular to the grain of 7.17 MPa (Pranata and Suryoatmono 2013), and is included in Grade Class II, therefore it can be used as a structural member of building structures (SNI 7973:2013, FPL 2021). Several wood structure codes, namely NDS 2024 (AWC 2024), SNI 7973:2013, and Eurocode 5 (CEN 2008) provide guidance on design of beams, columns, and connections. The results of the bolted beam-to-column timber connections investigated in this research can be a reference for predicting the behavior of such connections. Tab. 5 summarizes all the properties of the bolted beam-to-column timber connections obtained in this study.

Tab. 5: Results obtained from investigation of behavior of bolted beam-to-column timber connections.

Type of connections	Type 1		Type 2	
Specimen	BC32.10	BC32.12	BC33.10	BC33.12
Bolt's diameter	10 mm	12 mm	10 mm	12 mm
Strength (kN.m)	2.76	3.39	2.70	4.28
Initial rotational stiffness (N/mm)	714.49	1052.88	1260.05	2341.27
Energy dissipation (J)	156.98	147.25	172.45	163.38
Ductility ratio (-)	1.84	2.19	1.65	2.06

Each value in the table is the average of three specimens. Connections with larger diameter (12 mm) perform better than connections with smaller diameter (10 mm), in terms of higher initial stiffness, strength, and ductility ratio. It should be noted, however, that this is not the case

if the energy dissipation is considered where connections with smaller diameter have higher energy dissipation, although the difference is not significant. Therefore, this exception may be due to the randomness mechanical properties of the wood. Comparing the performances of connection type 1 and connection type 2 by considering the connections with bolt diameter of 12 mm only, it is very clear that connection type 2 performs better than connections type 1 in three aspects (much higher initial stiffness, strength, and energy dissipation). This is obvious because connection type 2 has more bolts than connection type 1. The ductility ratio of connection type 2 is only slightly smaller than that of connection type 1 and again it is considered due to the randomness mechanical properties of the wood. By considering the connections with bolt diameter of 10 mm only, comparing the performances of connection type 1 and connection type 2 leads to conclusion that connection type 2 performs better than connections type 1 in terms of much higher initial stiffness and energy dissipation. The ductility ratio and strength of connection type 2, however, are smaller than those of connection type 1. Again, because the differences are very small, it is considered due to the randomness mechanical properties of the wood material that come from nature.

## **CONCLUSIONS**

Two types of bolted beam-to-column timber connections with double steel plates have been tested experimentally, namely the ones with more bolts in the column and the ones with the same number of bolts in the column and the beam. For each type of connection, bolt of 10-mm diameter and 12-mm diameter have been used. From studying the behavior of each type of the connection, it can be concluded that connection type 2 in general performs better than connection type 1 in terms of initial stiffness, strength, ductility ratio, and energy dissipation.

Precautions have to made, however, that the failure modes of connection type 2 are split in the column along the bolt line. This type of failure is not expected in the design of earthquake resistant buildings. In such case, connection type 1 is preferable where the failure mode is split in the bolt line of the beam. Both types of connections show relatively high ductility ratios and energy dissipation. Regarding the effect of bolt diameter, it can be concluded that in general the connections with larger diameter perform better than connections with smaller diameter.

## **ACKNOWLEDGMENTS**

This research was funded by the Internal Scheme funded by the Research and Community Service Institute of Maranatha Christian University, fiscal year of 2025.

## **REFERENCES**

1. ASTM D5764: 2018 standard test method for evaluating dowel-bearing strength of wood and wood-based products.

2. AMERICAN WOOD COUNCIL (2024): The 2024 national design specification for wood construction, American Wood Council Wood Design Standards Committee, United States of America.
3. BASZEN, M., MIEDZIALOWSKI, C. (2019): Impact of semi-rigid joints in light-wood framed structures on the serviceability limit state. In: IOP Conference Series: Materials Science and Engineering 471, 112086.
4. CASCIATI, S. (2007): Nonlinear aspects of energy dissipation in wood-panel joints. In: Earthquake Engineering and Engineering Vibration 6 (3), 259–268 pp.
5. EN 26891: 1991 Timber structures. Joint made with mechanical fasteners. General principles for the determination of strength and deformation characteristics.
6. Eurocode 5: 2008: Design of timber structures.
7. FAIRWEATHER, R.H. (1992): Beam column connections for multi-storey timber buildings, Master Theses, University of Canterbury, New Zealand. 99 pp.
8. FOREST PRODUCT LABORATORY (2021): Wood handbook: wood as an engineering material, General Technical Report FPL-GTR-190, Forest Product Laboratory, United States Department of Agriculture. 5-21 pp.
9. GOODNO, B.J., GERE, J.M. (2021): Mechanics of materials 9th edition, Publisher Cengage. 190 pp.
10. GUO, J. & SHU, Z. (2019): Theoretical evaluation of moment resistance for bolted timber connections. In: 3rd International Conference on Building Materials and Materials Engineering (ICBMM 2019) 303, Lisbon, Portugal, September 25-27. 03003.
11. HIBBELER, R.C. (2023): Mechanics of materials 11th Edition. Published by Pearson. 92 pp.
12. HUNG TA, Co., Ltd. (2008): HT-9501 Electro-hydraulic servo universal testing machines, Hung Ta Instrument Co. Ltd., Thailand. 9 pp.
13. HWANG, J.K., KWAK, S. & KWAK, J.H. (2008): Resisting capacity of Korean traditional wooden structural systems subjected to static loading. In: Structural Engineering and Mechanics 30 (3), 297-316 pp.
14. MEHRA, S., O'CEALLAIGH, C., SOTAYO, A., GUAN, Z. & HARTE, A.M. (2022): Experimental investigation of the moment-rotation behaviour of beam-column connections produced using compressed wood connectors. In: Construction and Building Materials 331, 127327.
15. MEHRA, S., MOHSENI, I., O'CEALLAIGH, C., GUAN, Z., SOTAYO, A., HARTE, A.M. (2019): Moment-rotation behaviour of beam-column connections fastened using compressed wood connectors. In: Proceedings of the 2019 Society of Wood Science and Technology International Convention, October 20-25, 2019, California, USA, 231 pp.
16. MUNOZ, W., MOHAMMAD, M., SALENIKOVICH, A. & QUENNEVILLE, P. (2008): Yield point and ductility of timber assemblies: A need for a harmonised approach. In: Annual Conference of the Canadian Society for Civil Engineering 2008, June 10-13, 2008, Quebec City, Quebec, Canada. 1146-1155 pp.
17. NEUSCH, M., SANDANUS, J. & FREUDENBERGER, K. (2022). Experimental verification of the modern semi-rigid timber connections: In: Wood Research 67(6), 1005-1016 pp.

18. PADALU, P.K.V.R. & SURANA, M. (2023): An overview of performance-based seismic design framework for reinforced concrete frame buildings. In: Iranian Journal of Science and Technology 48, 635-667 pp.
19. PONZO, F.C., ANTONIO, D.C., NICLA, L. & NIGRO, D. (2021): Experimental estimation of energy dissipated by multistorey post-tensioned timber framed buildings with anti-seismic dissipative devices. In: Sustainable Structures 1(2), 000007.
20. PRANATA, Y.A. & SURYOATMONO, B. (2024): Experimental tests of red meranti (*shorea spp.*) dowel bearing strength at an angle to the grain. In: Wood Research 69 (3), 369-375 pp.
21. PRANATA, Y.A. & SURYOATMONO, B. (2013): Nonlinear finite element modeling of red meranti compression at an angle to the grain. In: Journal Engineering and Technological Science 45(3), 222-240 pp.
22. REBOUCAS, A.S., MEHDIPOUR, Z., BRANCO, J.M. & LOURENCO, P.B. (2022): Ductile moment-resisting timber connections: a review. In: Buildings 12 (2), 240.
23. SANTANA, C.L.O. & MASCIA, N.T. (2009): Wooden framed structures with semi-rigid connections: Quantitative approach focused on design needs. In: Structural Engineering and Mechanics 31(3), 315-331 pp.
24. SNI 7973, 2013: Design specifications for wood construction. National Standardization Agency, Indonesia.
25. SOLARINO, F., GIRESINI, L., CHANG, W. & HUANG, H. (2017): Experimental tests on a dowel-type timber connection and validation of numerical models. In: Buildings 7(4), 116.
26. VILGUTS, A., NESHEIM, S.O., STAMATOPOULOS, H., MALO, K.A. (2022): A study on beam-to-column moment-resisting timber connections under service load, comparing full-scale connection testing and mock-up frame assembly. In: European Journal of Wood and Wood Products 80, 753–770 pp.

YOSAFAT AJI PRANATA\*  
UNIVERSITAS KRISTEN MARANATHA  
FACULTY OF SMART TECHNOLOGY AND ENGINEERING  
MASTER PROGRAM IN CIVIL ENGINEERING  
JL. SURIA SUMANTRI 65, BANDUNG, 40164  
WEST JAVA, INDONESIA  
\*Corresponding author: yosafat.ap@gmail.com

BAMBANG SURYOATMONO  
UNIVERSITAS KATOLIK PARAHYANGAN  
FACULTY OF ENGINEERING  
DOCTORAL PROGRAM IN CIVIL ENGINEERING  
JL. CIUMBULEUIT 94, BANDUNG, 40161  
WEST JAVA, INDONESIA